Estimation of Multi-Directional Cyclic Shear-Induced Pore Water Pressure on Clays with a Wide Range of Plasticity Indices

Hiroshi Matsuda[1], Tran Thanh Nhan[1,2], Hidemasa Sato[1,3]
[1]Yamaguchi University, 2-16-1 Tokiwadai, Ube, Yamaguchi 755-8611, Japan
[2]Hue University of Sciences, 77 Nguyen Hue, Hue City, Vietnam
[3] Fukken Co. Ltd., 2-10-11 Hikarimachi, Higashi-ku, Hiroshima, Japan
hmatsuda@yamaguchi-u.ac.jp; nhan@yamaguchi-u.ac.jp; f16624@fukken.co.jp

Abstract - To develop an estimation method of multi-directional cyclic shear-induced pore water pressure on clays with a wide range of plasticity indices, normally consolidated specimens of Kaolinite clay, Tokyo bay clay and Kitakyushu clay were subjected to the uni-directional and multi-directional cyclic simple shears under the undrained condition. Then firstly, the effects of cyclic shear direction on the pore water pressure accumulation and secondly, the relationships between the plasticity index of clay and the pore water pressure accumulated during cyclic shear were investigated. In conclusion, it is clarified that when a saturated clay is subjected to uni-directional or multi-directional cyclic simple shear under the undrained condition, the pore water pressure induced by multi-directional cyclic shear increases considerably larger than those generated by the uni-directional one and such a tendency is seen in clays with a wide range of the plasticity indices. The plasticity index of clayey soil significantly affects the pore water pressure generation and the higher the plasticity index of soil, the slower the rate of pore water pressure accumulation which leads to the smaller pore water pressure, irrespective of cyclic shearing conditions. A pore water pressure model was developed by incorporating the plasticity index as an experimental constant and the applicability of this model was confirmed.

Keywords: Clay, cyclic shear, plasticity index, pore water pressure, undrained

1. Introduction

When a saturated soil deposit is subjected to cyclic shear under the undrained conditions such as a short-term cyclic loading of earthquakes or the low permeability of clayey layers, the pore water pressure is produced which is commonly called as cyclic shear-induced pore water pressure, and such a pore water pressure increases leading to the decrease in the effective stress. Because the cyclic shear-induced pore water pressure accumulation itself relates to the cyclic degradation and significantly affects the cyclic resistance of the soil, the development of pore water pressure accumulation is therefore considered as an important parameter when estimating the cyclic behaviour of soil deposits under undrained cyclic loading. In addition, the dissipation of the residual pore water pressure after cyclic loading results in considerable instantaneous and long-term settlements which have been observed as a post-earthquake settlement after major earthquakes, such as Hyogo-ken Nanbu Earthquake in 1995 [1] or the Tohoku Earthquake in 2011 [2].

For saturated sand and cohesionless soils, the problems regarding the development of pore water pressure accumulation have been extensively studied by a number of researchers and models which are commonly in connection with the mechanism of soil liquefaction were developed [3-6]. Because clayey soils which are believed to be relatively stable compared with sandy soils [7-10], in spite of many systematic researches, studies on the cyclic shear-induced pore water pressure have not reached the same goals [11,12]. In addition, since the inter-particle forces which govern the complex pore water pressure response of clay microstructure are still insufficiently clarified, the "curve-fitting" method with the usage of suitable coefficients seems to be the only appropriate approach for effective modelling of the pore water pressure generation. Among which, the models proposed for the case of cyclic strain-controlled loading such as Ohara et al. [13]; Ohara and Matsuda [14], Matasovic and Vucetic [11,15] can be listed.

In this study, normally consolidated specimens of Kaolinite clay, Tokyo bay clay and Kitakyushu clay were tested under undrained uni-directional and multi-directional cyclic simple shears and the effects of undrained cyclic shearing conditions including cyclic shear direction, cyclic shear strain amplitude, and the plasticity of soils on the accumulation of pore water pressure were observed. Then a model of the cyclic shear-induced pore water pressure accumulation was

developed and the applicability of this model was confirmed by applying to other clayey soils with different plasticity indices.

2. Undrained Uni-Directional and Multi-Directional Cyclic Simple Shear Tests on Clays with Different Plasticity Indices

2.1. Test apparatus

Fig. 1 shows the photo and outline of the multi-directional cyclic simple shear test apparatus. This apparatus can give any types of cyclic displacement at the bottom of specimen from two orthogonal directions by using the electro-hydraulic servo system. A predetermined vertical stress can be applied to the specimen by the aero-servo system. The shear box is the Kjellman type in which the specimens were enclosed in a rubber membrane. The flank of the membrane-enclosed specimen is surrounded by a stack of 15, 17 and 20 acrylic rings for the case of Kaolin, Tokyo bay clay and Kitakyushu clay, respectively. Each acrylic ring has 75.4 mm in inside diameter and 2 mm in thickness. In this condition, the specimen is prevented from the radial deformation but permitted the simple shear deformation during cyclic shearing.
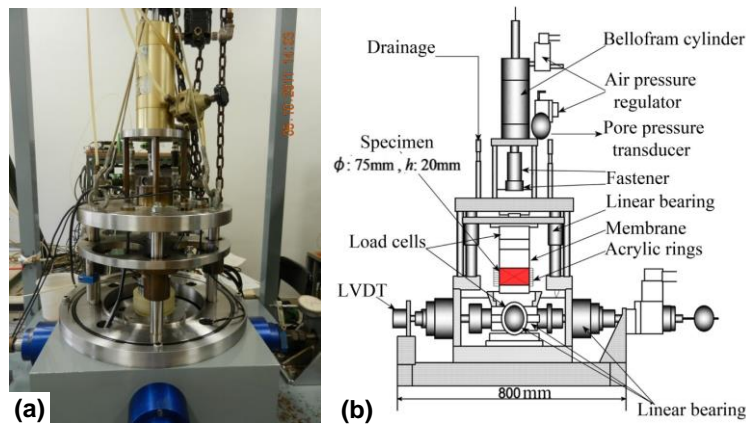

Fig. 1: (a) Photo and (b) outline of the multi-directional cyclic simple shear test apparatus.

2.2. Samples and specimen

The soils used in this study are Kaolinite clay, Tokyo bay clay and Kitakyushu clay. The grain size distribution curves and several index properties of these soils are shown in Fig. 2 and Table 1, respectively.
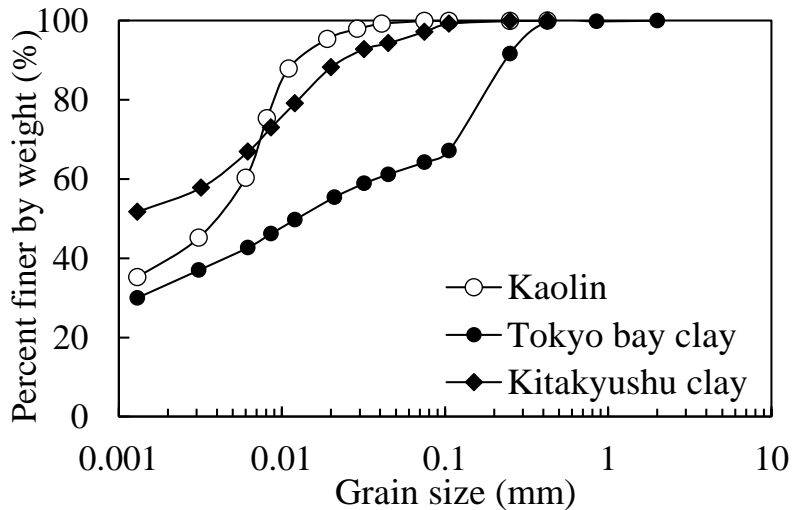

Fig. 2: Grain size distributions of soils.

Table 1: Index properties of soils.

Properties	Kaolin	Tokyo bay clay	Kitakyushu clay
Specific gravity, G_s	2.71	2.77	2.63
Liquid limit, w_L (%)	47.8	66.6	98.0
Plastic limit, w_P (%)	22.3	25.0	34.2
Plasticity index, I_p	25.5	41.6	63.8
Compression index, C_c	0.31	0.46	0.60

In order to prepare the test specimen, samples were firstly mixed with the de-aired water to form slurries having a water content of about $1.5 \times w_L$ which were separately kept in big tanks under the constant water content. Secondly, the slurry of each clay was taken out to a smaller box for one day before being de-aired in the vacuum cell with tamping. Thirdly, the slurry was poured into the shear box of the test apparatus. The slurry was pre-consolidated under the vertical stress $\sigma_{v0} = 49$ kPa until the pore water pressure inside the soil specimen is dissipated. After the pre-consolidation, the dimension of specimen was 75 mm in diameter and about 20 mm in height with the initial void ratio was about $e_0 = 1.11$-1.19, 1.20-1.37 and 1.61-1.81 for Kaolin, Tokyo bay clay and Kitakyushu clay, respectively. Since the pore pressure coefficient of soil specimen before undrained cyclic shear was confirmed as B-value > 0.95, the required degree of saturation can be satisfied.

2.3. Test procedures and conditions

After pre-consolidation is completed, the soil specimen was subjected to the strain-controlled cyclic simple shear under the undrained condition for predetermined number of cycles (n), shear strain amplitude (γ) and cyclic shear direction.

Table 2: Experimental Conditions.

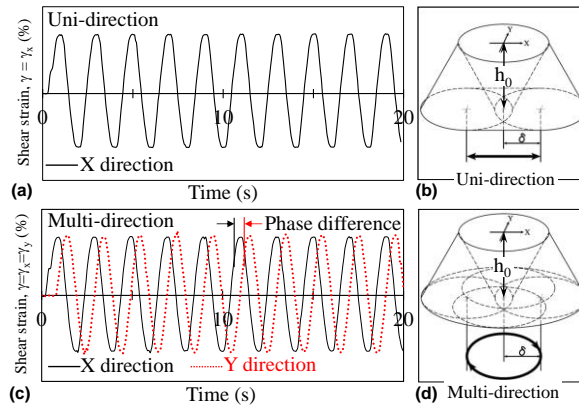| Uni-directional cyclic simple shear tests			
Period T (s)	Number of cycles n	Soil	Shear strain amplitude γ (%)
2	200	Kaolin	0.1, 0.2, 0.3, 0.4, 0.5, 0.6, 0.8, 1.0, 1.2, 2.0
		Tokyo bay clay	0.1, 0.2, 0.4, 0.8, 1.0, 1.2, 2.0
		Kitakyushu clay	0.1, 0.2, 0.4, 0.8, 1.0, 1.2, 2.0
Multi-directional cyclic simple shear tests			
Period T (s)	Number of cycles n	Soil	Phase difference θ (°) Shear strain amplitude γ (%)
2	200	Kaolin	20, 45, 70, 90 0.1, 0.2, 0.3, 0.4, 0.5, 0.6, 0.8, 1.0, 1.2, 2.0
		Tokyo bay clay	20, 45, 70, 90 0.05, 0.1, 0.2, 0.4, 0.8, 1.0, 1.2, 2.0
		Kitakyushu clay	45, 90 0.05, 0.1, 0.2, 0.4, 0.8, 1.0, 1.2, 2.0

Fig. 3: Typical records of cyclic shear waves and respective deformations of specimen under (a,b) uni-directional and (c,d) multi-directional cyclic shears.

Experimental conditions are shown in Table 2 in detail. The cyclic shear direction was changed as uni-direction (only X direction) and multi-direction in which the specimen was subjected to the cyclic shear deformation in X and Y directions independently, with the phase difference $\theta = 20^0$, 45^0, 70^0 and 90^0. The shear strain amplitude was also changed in the range from $\gamma = 0.05\%$ to 2.0% and the number of cycles was fixed as $n = 200$. Each wave form of the cyclic shear strain is sinusoidal (two way cyclic strain) with the period 2 s. The typical records of cyclic shear strains and the respective deformation of specimen are shown in Figs. 3(a-d) for both cases of uni-directional and multi-directional cyclic shears. In this study, the shear strain amplitude is defined as a ratio of the maximum horizontal displacement (δ) to the initial height (h_0) of the specimen. In uni-directional test, the shear strain was applied to the specimen only in X direction ($\gamma_x = \gamma$) (Figs. 3a and b) and so the orbit of cyclic shear strain forms a linear line (Fig. 3b). In multi-directional test (Figs. 3c and d), the cyclic shear was simultaneously applied to X direction (γ_x) and Y direction (γ_y) which are perpendicular to each other under the same shear strain amplitude ($\gamma_x = \gamma_y = \gamma$) with different phase differences. Then the orbits show the elliptical line for $0^0 < \theta < 90^0$ and the circle line for $\theta = 90^0$ which is commonly known as a gyratory cyclic shear (Fig. 3d).

3. Pore Water Pressure Accumulated in Clays with Different Plasticity Indices

3.1. Changes of pore water pressure in saturated clays subjected to undrained cyclic shear

As a result of undrained cyclic shear, pore water pressure (U_{dyn}) increases with the number of cycles. Typical changes of the pore water pressure ratio which is defined by U_{dyn}/σ'_{v0}, during undrained uni-directional cyclic shear and multi-directional cyclic shear ($\theta = 90^0$) with $\gamma = 0.1\%$, 0.4%, 1.0% and 2.0% are shown in Figs. 4(a), (b) and (c) for Kaolin, Tokyo bay clay and Kitakyushu clay, respectively. Where σ'_{v0} is the initial effective stress. The observed results of uni-directional tests in these figures are especially notified as "uni". From these figures, the effects of cyclic shear direction, shear strain amplitude and number of cycles on the pore water pressure accumulation can be confirmed for each clay. In addition, when comparing the results for different clays, it is clarified that under the same cyclic shear conditions, the higher the plasticity index of the soil, the slower the rate of pore water pressure development leading to the lower pore water pressure in Kitakyushu clay and Tokyo bay clay, compared with those in Kaolinite clay. For the case of shear strain amplitude of $\gamma = 0.1\%$, the pore water pressures in Kaolin evidently increase after several cycles of cyclic shear, while in Tokyo bay clay and Kitakyushu clay, the pore water pressures fluctuate around zero even after a long-term application of cyclic shear strain. Therefore, it is indicated that the plasticity index affects the generation and development of cyclic shear-induced pore water pressure in cohesive soils.
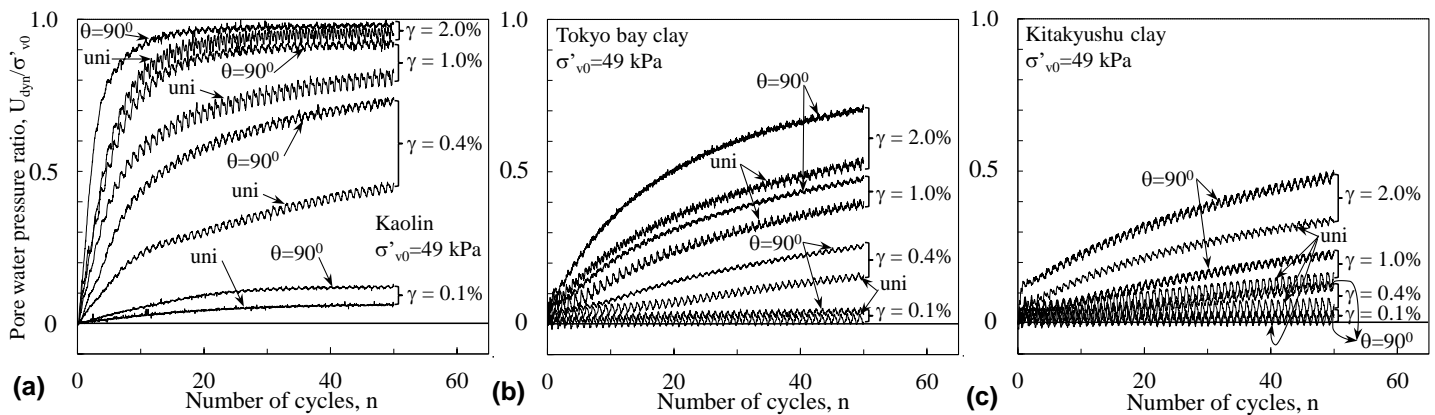

Fig. 4: The changes of U_{dyn}/σ'_{v0} in (a) Kaolin, (b) Tokyo bay clay and (c) Kitakyushu clay under undrained uni-directional and multi-directional cyclic shears ($\theta = 90^0$).

Furthermore, the cyclic stiffness and resistance of soil deposits are significantly affected by the pore water pressure, and also relations between the pore water pressure and the cyclic degradation in clayey soil have been confirmed [11,15]. Then the lower level of pore water pressure seems to show the higher cyclic resistance and the lower cyclic degradation under undrained uni-directional and multi-directional cyclic shears.

3.2. Equation showing the cyclic pore water pressure changes during undrained cyclic simple shear

Ohara et al. [13] indicated that when normally consolidated Kaolin is subjected to undrained cyclic simple shear, U_{dyn} increases with n. The authors then proposed an equation showing the relations between U_{dyn}/σ'_{v0} and n as follows:

$$\frac{U_{dyn}}{\sigma'_{v0}} = \frac{n}{\alpha + \beta n} \tag{1}$$

where α and β are experimental parameters which depend on the cyclic shear strain amplitude and can be defined as:

$$\alpha = A(\gamma)^m \tag{2}$$

$$\beta = \frac{\gamma}{B + C\gamma} \tag{3}$$

The constants A, B, C and m in Eqs. (2) and (3) can be determined by the curve-fitting method. Thereafter, Eq. (1) was applied to estimate the cyclic pore water pressure accumulation. Eq. (1) also has been used to predict the post-cyclic settlement [1,14,16].

3.3. Estimation of the pore water pressure accumulation in clays with different plasticity indices

Relationships between U_{dyn}/σ'_{v0} and n are plotted in Fig. 5 for three kinds of clay when subjected to undrained uni-directional and multi-directional cyclic shears with a wide range of shear strain amplitudes. Symbols in these figures show the observed results, solid curves correspond to the calculated ones by using Eq. (1). Reasonable agreements between them are observed.
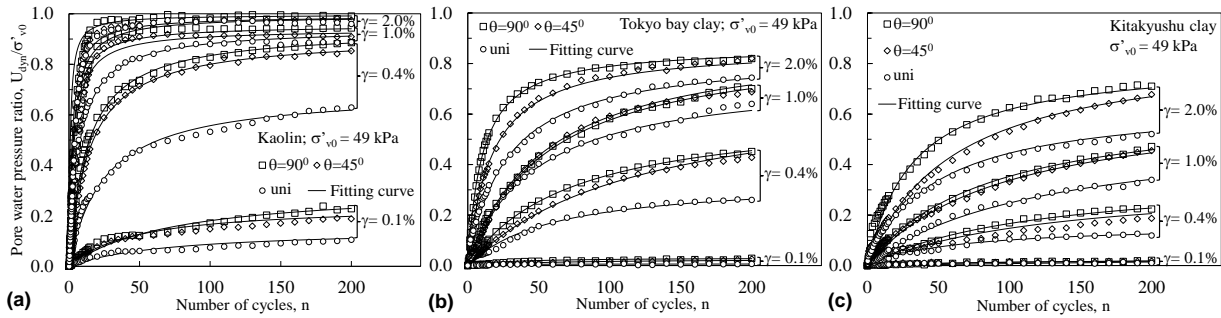

Fig. 5: Relations between U_{dyn}/σ'_{v0} and n for (a) Kaolin, (b) Tokyo bay clay and (c) Kitakyushu clay subjected to uni-directional and multi-directional cyclic shears.

In this study, by using the curve-fitting method, the experimental parameters α and β (or A, B, C and m) in Eq. (1) were determined for the clays concerned, then the cyclic shear-induced pore water pressure can be estimated for both uni-directional and multi-directional cyclic shears. The changes of α and β with γ are plotted in Figs. 6 and 7, respectively. The obtained values of A, B, C and m are shown in Table 3.
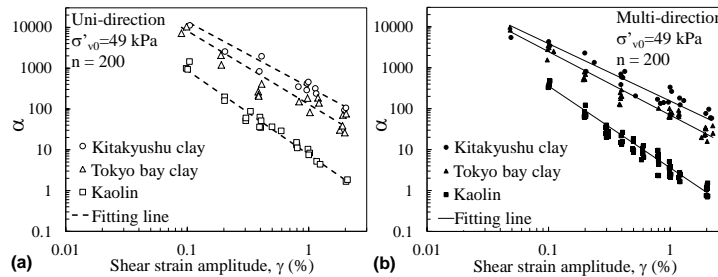

Fig. 6: Relations between α and γ for clays under (a) uni-directional and (b) multi-directional cyclic shears.

The comparisons between experimental results and calculated ones for the pore water pressure induced by uni-directional and multi-directional cyclic shears are shown in Fig. 8 for each clay. Symbols in this figure show experimental results, and solid and dashed lines correspond to the calculated ones by using Eq. (1), where the values of A, B, C and m in Table 3 were used. Reasonable agreements between them are seen and therefore the applicability of the values in Table 3 is confirmed. In this figure, the changes in U_{dyn}/σ'_{v0} are similar to those in Figs. 4 and 5 in which the pore water pressure has a tendency to increase with the shear strain amplitude.
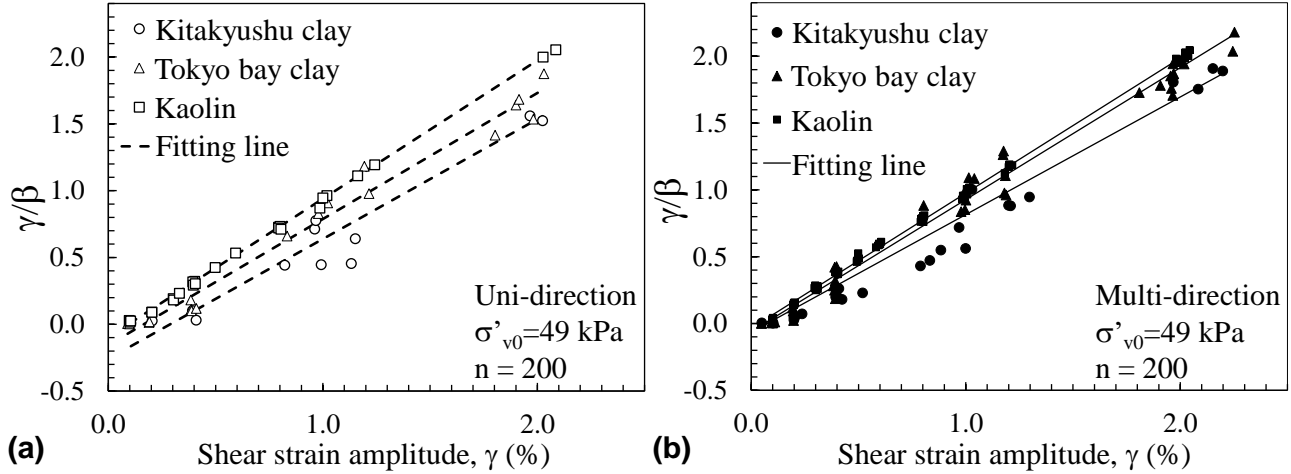

(a) **(b)**

Fig. 7: Relations between β and γ for different clays under (a) uni-directional and (b) multi-directional cyclic shears.

Table 3: Experimental constants A, B, C and m.

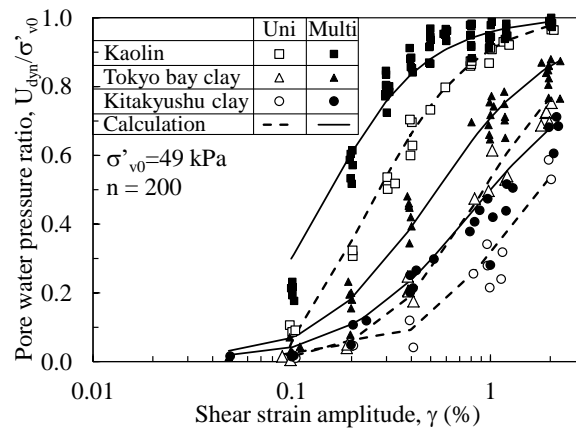| Cyclic shear direction	Soil	A	B	C	m
Uni-direction	Kaolin	7.6	-0.0960	1.0353	-2.065
	Tokyo bay clay	130.0	-0.1553	0.9700	-1.800
	Kitakyushu clay	300.0	-0.2400	0.8500	-1.600
Multi-direction	Kaolin	3.6	-0.0354	1.0110	-1.998
	Tokyo bay clay	65.0	-0.0600	0.9800	-1.550
	Kitakyushu clay	155.0	-0.0650	0.8800	-1.400

Fig. 8: Relations between U_{dyn}/σ'_{v0} and γ for different clays subjected to uni-directional and multi-directional cyclic shears.

3.4. Estimation of the cyclic shear-induced pore water pressure concerning the effect of plasticity index

In order to incorporating the plasticity index into Eq. (1), relationships between the experimental constants A, B, C, m and I_p are plotted in Fig. 9 in which the fitting lines are also shown following the equation in Table 4.

Relations between U_{dyn}/σ'_{v0} and the logarithm of γ are shown in Fig. 10 for clays subjected to uni-directional and multi-directional cyclic shears. Symbols in this figure show experimental results, and solid and dashed curves correspond to the calculated ones by using Eq. (1) where the experimental constants A, B, C and m were determined by the correlations in Table 4. Calculated results agree well with the observed ones. Therefore, by incorporating the plasticity index into Eq. (1) following the equations in Table 4, Eq. (1) is possibly to be used for estimating the cyclic shear-induced pore water pressure accumulation for any kinds of clay when subjected to undrained uni-directional and multi-directional cyclic shears.
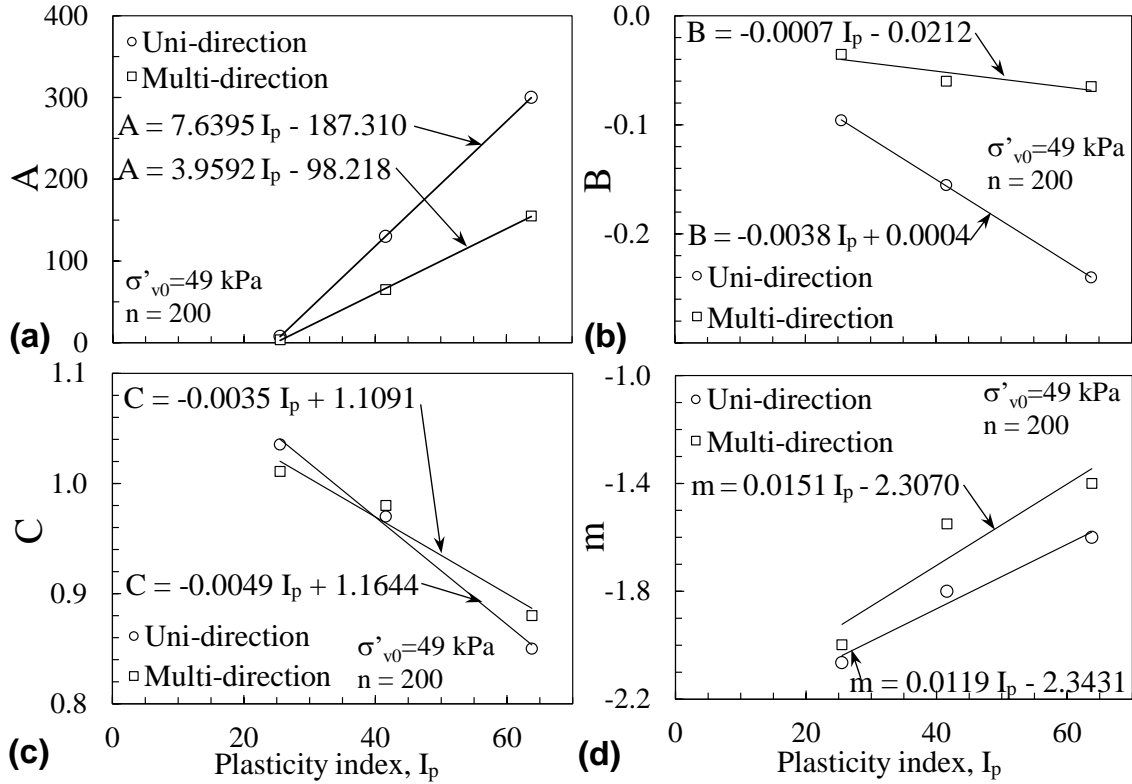

Fig. 9: The changes of A, B, C and m with I_p.
Table 4: Experimental constants A, B, C and m in relation to I_p.

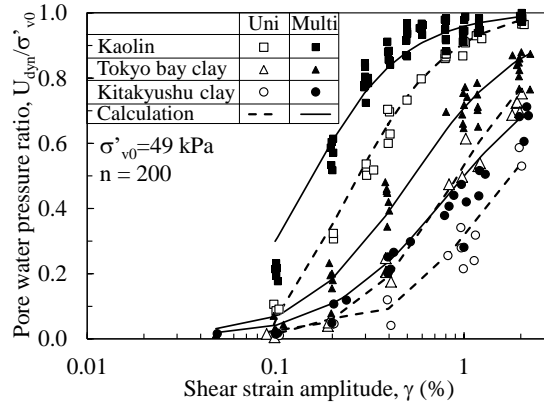| Experimental	Cyclic shear direction	
constants	Uni-direction	Multi-direction
A	$A = 7.6395 I_p - 187.310$	$A = 3.9592 I_p - 98.218$
B	$B = -0.0038 I_p + 0.0004$	$B = -0.0007 I_p - 0.0212$
C	$C = -0.0049 I_p + 1.1644$	$C = -0.0035 I_p + 1.1091$
m	$m = 0.0119 I_p - 2.3431$	$m = 0.0151 I_p - 2.3070$

Fig. 10: Comparison between experimental data and calculated results for the relations of U_{dyn}/σ'_{v0} versus γ under uni-directional and multi-directional cyclic shears including the effect of the plasticity index.

4. Conclusions

When saturated clays subjected to undrained cyclic simple shear, the pore water pressure induced by multi-directional cyclic shear increases considerably higher than those generated by the uni-directional one and the same tendency is seen in clays with a wide range of the plasticity indices.

Also, the plasticity of clayey soil itself significantly affects the pore water pressure generation during undrained uni-directional and multi-directional cyclic shears. The higher the plasticity index of the soil, the slower the rate of cyclic shear-induced pore water pressure accumulation which leads to the lower level of pore water pressure accumulation, irrespective of cyclic shearing conditions.

A pore water pressure model was developed by incorporating the effect of the plasticity index as correlations with its four experimental constants. The applicability of this model for the pore water pressure accumulation induced by undrained uni-directional and multi-directional cyclic shears was then confirmed.

Acknowledgements

References

[1] H. Matsuda, "Estimation of post-earthquake settlement-time relations of clay layers," *J. JSCE Division C*, vol. 568, no. III-39, pp. 41-48, 1997.

[2] K. Konagai, T. Kiyota, S. Suyama, T. Asakura, K. Shibuya, and C. Eto, "Maps of soil subsidence for Tokyo bay shore areas liquefied in the March 11th, 2011 off the Pacific Coast of Tohoku Earthquake," *Soil Dynamics and Earthquake Engineering*, vol. 53, pp. 240-253, 2013.

[3] R. Pyke, H. B. Seed, and C. K. Chan, "Settlement of sands under multidirectional shaking," *J. Geotechnical Eng.*, vol. 101, no. GT4, pp. 379-398, 1975.

[4] K. Ishihara and M. Yoshimine, "Evaluation of settlements in sand deposits following liquefaction during earthquakes," *Soils and Foundations*, vol. 32, no. 1, pp. 173-188, 1992.

[5] H. Matsuda, H. Shinozaki, N. Okada, K. Takamiya, and K. Shinyama, "Effects of multi-directional cyclic shear on the post-earthquake settlement of ground," in *Proceedings of 13th World Conference on Earthquake Engineering*, Vancouver, BC, 2004, no. 2890.

[6] H. Matsuda, P. H. Andre, R. Ishikura, and S. Kawahara, "Effective stress change and post-earthquake settlement properties of granular materials subjected to multi-directional cyclic simple shear," *Soils and Foundations*, vol. 51, no. 5, pp. 873-884, 2011.

[7] M. Hyodo, Y. Yamamoto, and M. Sugiyama, "Undrained cyclic shear behaviour of normally consolidated clay subjected to initial static shear stress," *Soils and Foundations*, vol. 34, no. 4, pp. 1-11, 1994.

[8] M. Hyodo, A. F. L. Hyde, Y. Yamamoto, and T. Fujii, "Cyclic shear strength of undisturbed and remoulded marine clays," *Soils and Foundations*, vol. 39, no. 2, pp. 45-58, 1999.

[9] K. Yasuhara, K. Hirao, and A. F. L. Hyde, "Effects of cyclic loading on undrained strength and compressibility of clay," *Soils and Foundations*, vol. 32, no. 1, pp. 100-116, 1992.

[10] K. Yasuhara, S. Murakami, N. Toyota, and A. F. L. Hyde, "Settlements in fine-grained soils under cyclic loading," *Soils and Foundations*, vol. 41, no. 6, pp. 25-36, 2001.

[11] N. Matasovic and M. Vucetic, "A pore pressure model for cyclic straining of clay," *Soils and Foundations*, vol. 32, no. 3, pp. 156-173, 1992.

[12] H. Yildirim and H. Ersan, "Settlements under consecutive series of cyclic loading," *Soil Dynamics and Earthquake Engineering*, vol. 27, no. 6, pp. 577-585, 2007.

[13] S. Ohara, H. Matsuda and Y. Kondo, "Cyclic simple shear tests on saturated clay with drainage," *J. JSCE Division C*, vol. 352, no. III-2, pp. 149-158, 1984.

[14] S. Ohara and H. Matsuda, "Study on the settlement of saturated clay layer induced by cyclic shear," *Soils and Foundations*, vol. 28, no. 3, pp. 103-113, 1988.

[15] N. Matasovic and M. Vucetic, "Generalized cyclic degradation pore pressure generation model for clays," *J. Geotechnical Eng.*, vol. 121, no. 1, pp. 33-42, 1995.

[16] H. Matsuda and H. Nagira, "Decrease in effective stress and reconsolidation of saturated clay induced by cyclic shear," *J. JSCE Division C*, vol. 659, no. III-52, pp. 63-75, 2000.